Thermochemistry and Kinetics of the Reaction of 1-Methylallyl Radicals with Molecular Oxygen

Vadim D. Knyazev* and Irene R. Slagle*

Department of Chemistry, The Catholic University of America, Washington, D.C. 20064

Received: July 8, 1998; In Final Form: September 1, 1998

The kinetics of the reaction $CH_3CHCHCH_2 + O_2 \rightleftarrows CH_3CHCHCH_2O_2$ has been studied using laser photolysis/photoionization mass spectrometry. Room-temperature decay constants of the $CH_3CHCHCH_2$ radical were determined in time-resolved experiments as a function of bath gas density ([He] = (3−24) × 10^{16} molecule cm^{-3}. The rate constants are in the falloff region under the conditions of the experiments. Relaxation to equilibrium in the addition step of the reaction was monitored within the temperature range 345−390 K. Equilibrium constants were determined as a function of temperature and used to obtain the enthalpy of reaction 1. At high temperatures (600−700 K), no reaction of $CH_3CHCHCH_2$ with molecular oxygen could be observed and upper limits to the rate constants were determined (1×10^{-16} cm^3 $molecule^{-1}$ s^{-1} at 600 K and 2×10^{-16} cm^3 $molecule^{-1}$ s^{-1} at 700 K). Structures, vibrational frequencies, and energies of several conformations of $CH_3CHCHCH_2$, $CH_3CHCHCH_2O_2$, and $CH_3CH(OO)CHCH_2$ were calculated using ab initio UHF and MP2 methods. The results were used to calculate the entropy changes of the addition reaction. These entropy changes combined with the experimentally determined equilibrium constants resulted in the average R−O_2 bond energy for terminal and nonterminal addition: $\Delta H^o_{298} = 82.6 \pm 5.3$ kJ mol^{-1}. Earlier experimental results on the kinetics of relaxation to equilibrium in the reaction of allyl radical with O_2 are reanalyzed using an improved kinetic mechanism which accounts for heterogeneous wall decay of the $CH_2CHCH_2O_2$ adduct. The corrected value of the CH_2CHCH_2−O_2 bond energy (77.0 kJ mol^{-1}) is determined from the reinterpreted data.

I. Introduction

Oxidation of polyatomic free radicals (R) by molecular oxygen is a key elementary step in combustion processes. While the state of knowledge of the reactions of alkyl radicals with O_2 is still far from being satisfactory, experimental information on the kinetics and mechanisms of analogous reactions of stabilized alkenyl radicals with oxygen is even more sparse. At the same time, such information is important for understanding the chemistry of hydrocarbon combustion. Alkenyl radicals are easily formed via attack of a reactive intermediate such as OH or H on the H atom in the β-position to the double bond in alkenes. The corresponding activation energy is lowered due to electron delocalization on the radical formed. The stability and low reactivity of these alkenyl radicals have been linked to the antiknock effect of fuel additives such as ethyl *tert*-butyl ether (ETBE).[1,2]

The R−O_2 bond energy for the simplest of the stabilized alkenyl radicals, allyl (CH_2CHCH_2), has been reported by Ruiz et al.,[3] Morgan et al.,[4] and Slagle et al.[5] It has been shown by Walker and co-workers (refs 6 and 7 and references therein) that, at high temperatures, where the equilibrium in the R+O_2 $\rightleftarrows$ RO_2 addition reaction is shifted to the left, the rate constants of the CH_2CHCH_2+O_2 → products reaction are significantly lower than those observed in the case of alkyl radicals. Baldwin et al.[8] and Lodhi and Walker[9] reported similarly low rate constants for the substituted allyl radicals, $CH_3CH_2CHCHCH_2$ and $CH_3CHCHCH_2$.

Here we report the results of an experimental investigation of the reaction

$$CH_3CHCHCH_2 + O_2 \rightleftarrows \text{products} \qquad (1)$$

over wide intervals of temperatures and pressures. The distinctly different behavior of reaction 1 in the low-, intermediate, and high-temperature regions is quantitatively characterized. Equilibrium constants of the addition step in reaction 1 were measured as a function of temperature. Properties of CH_3-$CHCHCH_2$, $CH_3CH(OO)CHCH_2$, and $CH_3CHCHCH_2O_2$ were determined in an ab initio study and used to calculate the entropies of these radicals. These calculated entropy values, together with the experimental equilibrium constants, were used to obtain the R−O_2 bond energy. Earlier results of Slagle et al.[5] on the relaxation to equilibrium in the reaction of allyl radicals with O_2 were reinterpreted using a corrected mechanism[10] which accounts for a possible wall loss of peroxy radicals.

II. Experimental Section

$CH_3CHCHCH_2$ radicals were produced at elevated temperatures by pulsed laser photolysis, and their decay was subsequently monitored in time-resolved experiments using photoionization mass spectrometry. Details of the experimental apparatus[11] used have been described before and so are only briefly reviewed here.

Pulsed unfocused 248- (or 193-) nm radiation (4 Hz) from a Lambda Physik EMG 201MSC excimer laser was directed along the axis of a heatable quartz reactor (1.05-cm i.d., coated with boron oxide[12]). Gas flowing through the tube at ≈4 m s^{-1} contained the radical precursor (<0.5%), molecular oxygen in varying concentrations, and an inert carrier gas (He) in large excess. The flowing gas was completely replaced between laser pulses.

10.1021/jp982923a CCC: $15.00
Published on Web 10/21/1998

Gas was sampled through a hole (0.04 cm diameter) in the side of the reactor and formed into a beam by a conical skimmer before the gas entered the vacuum chamber containing the photoionization mass spectrometer. As the gas beam traversed the ion source, a portion was photoionized and mass selected. $CH_3CHCHCH_2$ radicals were ionized using the light from a bromine resonance lamp (7.6−7.9 eV) with a sapphire window. Temporal ion signal profiles ($C_4H_7^+$, $m/e = 55$) were recorded on a multichannel scaler from a short time before each laser pulse up to 25 ms following the pulse. Data from 1 000 to 55 000 repetitions of the experiment were accumulated before the data were analyzed.

$CH_3CHCHCH_2$ radicals were produced by the pulsed, 193-nm or 248-nm laser photolysis of crotyl bromide

$$CH_3CHCHCH_2Br \xrightarrow{h\nu} CH_3CHCHCH_2 + Br, \quad (2)$$
$$\rightarrow \text{other products},$$

crotyl chloride

$$CH_3CHCHCH_2Cl \xrightarrow{h\nu} CH_3CHCHCH_2 + Cl, \quad (3)$$
$$\rightarrow \text{other products},$$

and 3-chloro-1-butene

$$CH_3CHClCHCH_2 \xrightarrow{h\nu} CH_3CHCHCH_2 + Cl, \quad (4)$$
$$\rightarrow \text{other products},$$

Initial conditions (precursor concentration and laser intensity) were selected to provide low radical concentrations ($\leq 10^{11}$ molecule cm^{-3}) such that reactions between radical products had negligible rates compared to those of the reactions of $CH_3CHCHCH_2$ with molecular oxygen.

The gases used were obtained from Aldrich (crotyl bromide, 85% (remainder 3-bromo-1-butene), crotyl chloride, 95% (predominantly trans, remainder 3-chloro-1-butene), and 3-chloro-1-butene, 98%) and Matheson (He, >99.995%; O_2, >99.6%). Precursors and oxygen were purified by vacuum distillation prior to use. Helium was used as provided.

III. Results

In the absence of molecular oxygen, the kinetics of the $CH_3CHCHCH_2$ radicals was that of an exponential decay with a first-order constant in the range 9−50 s^{-1}. This was attributed to the heterogeneous wall reaction:

$$CH_3CHCHCH_2 \rightarrow \text{heterogeneous loss} \quad (5)$$

The reaction with O_2 displayed distinctly different behavior in low (room temperature), intermediate, and high-temperature intervals. While it was possible to experimentally determine bimolecular rate constants of the reaction of $CH_3CHCHCH_2$ radicals with O_2 in the low-temperature region, the reaction exhibited nonexponential radical decay in an excess of molecular oxygen at intermediate temperatures. The observed decay curves could be fitted to a double-exponential function. This behavior is indicative of relaxation to an equilibrium of the type $R + O_2 \rightleftarrows RO_2$:

$$CH_3CHCHCH_2 + O_2 \rightleftarrows CH_3CHCHCH_2O_2 \quad (1a,-1a)$$

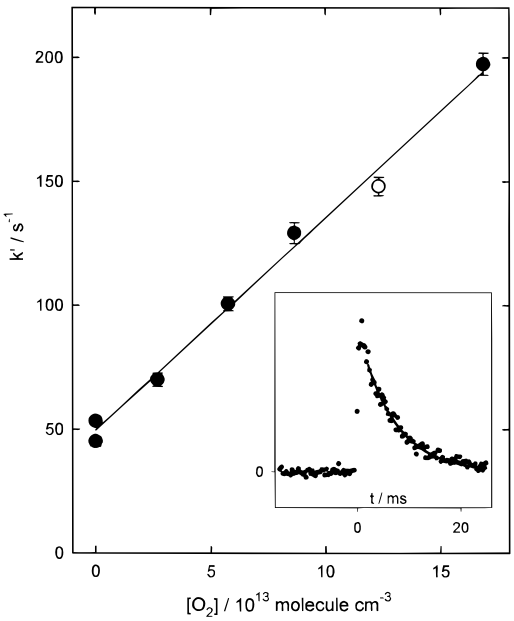

Figure 1. First-order $CH_3CHCHCH_2$ decay rate k' vs $[O_2]$. The intercept at $[O_2] = 0$ corresponds to the rate of heterogeneous decay of $CH_3CHCHCH_2$ radicals. $T = 300$ K, $[He] = 6.0 \times 10^{16}$ molecules cm^{-3}, $[CH_3CHCHCH_2Br] = 2.89 \times 10^{11}$ molecule cm^{-3}. The insert shows the recorded $CH_3CHCHCH_2$ decay profile (and exponential fit) for the conditions of the open plotted point: $[O_2] = 1.23 \times 10^{14}$ molecules cm^{-3}, $k' = 148.1 \pm 3.7$ s^{-1}.

At high temperatures, the equilibrium in reaction (1a,−1a) is shifted to the left and any possible overall reaction can only be due either to a further reaction of the $CH_3CHCHCH_2O_2$ adduct or to a direct abstraction reaction. No reaction with O_2 could be observed between 600 and 700 K which indicates that both of these processes are inefficient. An upper limit to the high-temperature rate constant was obtained.

III.1. Room-Temperature Reaction. At room temperature the decay of $CH_3CHCHCH_2$ radicals in an excess of O_2 was exponential. The experiments were conducted under pseudo-first-order conditions with $[O_2]$ in the range $(1.65-22.7) \times 10^{13}$ molecules cm^{-3}. The radical signal profiles were fit to an exponential function ($[R]_t = [R]_0 \exp(-k't)$) by using a nonlinear least-squares procedure. The pseudo-first-order radical decay constants, k', were obtained as a function of the concentration of molecular oxygen. The values of the second-order rate constant, k_1, were determined from the slopes of linear plots of k' vs $[O_2]$ (Figure 1). Experiments were performed to establish that decay constants did not depend on initial radical concentrations (provided that the concentration was kept low enough to ensure that radical−radical reactions had negligible rates compared to the reaction with O_2), radical precursor concentration, or photolyzing laser intensity and wavelength.

The room-temperature rate constants of reaction 1 were determined at $[He] = (3-24) \times 10^{16}$ atoms cm^{-3}. These bimolecular rate constants of the reactions of $CH_3CHCHCH_2$ radicals with molecular oxygen (interpreted as addition reaction 1a) exhibit a pronounced falloff behavior. The values of k_1 increase with pressure within the experimental pressure range (Figure 2). The conditions and results of these experiments are presented in Table 1.

III.2. High-Temperature Reaction. In the high-temperature region (600−700 K), no reaction of $CH_3CHCHCH_2$ radicals with molecular oxygen could be observed. When 248-nm photolysis with high laser intensity (58−23 mJ $pulse^{-1}$ cm^{-2}) was used, rates of radical decay increased slightly (up to 62

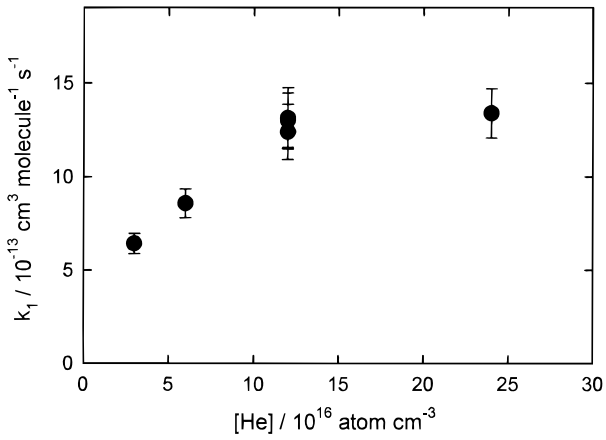

Figure 2. Falloff in k_1 at room temperature.

s^{-1} compared to the wall decay rate of 20 s^{-1}) when very high concentrations of molecular oxygen (up to 8.8×10^{16} molecules cm^{-3}) were added to the flow. However, such an increase was not observed when significantly lower laser intensities (0.7−2.8 mJ $pulse^{-1}$ cm^{-2}) were used. The upper limit values of k_1 (1×10^{-16} at 600 K and 2×10^{-16} at 700 K) were obtained by adding up to 10^{17} molecules cm^{-3} of O_2 (the concentration of He was reduced accordingly so that the total concentration of bath gas remains constant, Table 1). The slight increase of the radical decay rate in the presence of very large O_2 concentrations observed at high photolyzing laser intensity could be explained by the photolysis of small amounts of impurities contained in the molecular oxygen or by the effects of laser irradiation on the reactor walls in the presence of radical precursor and O_2. A more significant increase in decay rates upon the addition of O_2 was observed in experiments where more energetic 193-nm radiation was used. Such an increase similar to that observed in the study of the $(CH_3)_2CCl+O_2$ reaction[16] was attributed to a contribution from a reaction of $CH_3CHCHCH_2$ with the products of the photodissociation or electronic excitation[13] of O_2 by the 193-nm radiation at elevated temperatures. Conditions of experiments with low-intensity 248-nm photolysis which allowed an estimate of the upper limit of the rate constant for reaction 1 are listed in Table 1. The upper temperature limit of the experiments (700 K) was determined by the rapid increase with temperature of the ion signal background (which can be attributed to thermal decomposition of the radical precursor or ion fragmentation).

III.3. Intermediate Temperature Range. Determination of Equilibrium Constants. In the intermediate temperature range (345−390 K) the decay of $CH_3CHCHCH_2$ radicals in the presence of O_2 displays a nonexponential behavior, which can be fit with a double-exponential function. The kinetics of $CH_3CHCHCH_2$ decay was analyzed under the assumption that the following processes are important under these conditions: (1) heterogeneous loss of $CH_3CHCHCH_2$, reaction 5; (2) reversible addition of O_2, reaction (1a,−1a); (3) decay of the adduct, $CH_3CHCHCH_2O_2$, due to heterogeneous loss, which is described by a first-order rate constant k_d. The kinetics of the $CH_3CHCHCH_2$ radical signal $I(t)$ in such a system can be described by the following double-exponential expression:[10,14]

$$I(t) = I_1\exp(-\lambda_1 t) + I_2\exp(-\lambda_2 t) \qquad \text{(I)}$$

where

$$I_1 = I_0\frac{k_{1a}[O_2] + k_5 - \lambda_2}{\lambda_1 - \lambda_2}$$

$$I_2 = I_0 - I_1$$

$$\lambda_{1,2} = {}^1/_2(A \pm [A^2 - 4(k_{-1a}k_5 + k_{1a}[O_2]k_d + k_5k_d)]^{1/2})$$

$$A = k_{1a}[O_2] + k_{-1a} + k_5 + k_d$$

The values of k_5 were measured directly in the absence of O_2. The temporal profile of the $CH_3CHCHCH_2$ signal was fitted to formula I using k_{1a}, K_1, I_0, and k_d as adjustable parameters (here $K_1 = k_{1a}/k_{-1a}$ is the equilibrium constant of the reaction (1a,−1a), and I_0 is the signal value at $t = 0$). After the values of the above parameters were found, the fitting procedure was repeated several times with K_1 fixed at selected values in the vicinity of the best value, and the other three parameters floated. As a result the sum of squares of deviations was determined as a function of K_1 (with the three other parameters optimized) in the vicinity of its minimum and fitted with a parabolic function. From that information the experimental relative uncertainty ϵ of the fitted values of K_1 was determined using standard procedures[15] (also, see ref 16). In each experiment to determine the values of K_1 the data were accumulated until the criterion of $\epsilon \leq 10\%$ was satisfied. The equilibrium constants of reaction (1a,−1a) were determined as a function of temperature from 345 to 390 K. The conditions and results of these experiments are presented in Table 2. Equilibrium constants are plotted in Figure 3 as a function of temperature. The insert in Figure 3 presents an example of a double-exponential decay profile for reaction 1. Experiments were performed to establish that the K_1 values obtained did not depend on the nature or concentration of the radical precursor, the initial radical concentration, or the photolyzing laser wavelength or intensity. Experiments conducted with three different precursors of the $CH_3CHCHCH_2$ radical did not indicate any correlation between the values of K_1 and the type of precursor used (Table 2, Figure 3).

TABLE 1: Conditions and Results of Experiments to Measure $k_1(T[M])^e$

T (K)	$[M]/10^{16}$	$[\text{precursor}]/10^{11}$	L^a	$[O_2]/10^{13}$	$k_1/10^{-13}$ (cm^3 $molecule^{-1}$ s^{-1})	k_5 (s^{-1})
297	3.0	3.01	13	8.14−22.69	6.42 ± 0.54	48.6
300	6.0	2.89	13	2.68−16.86	8.58 ± 0.77	49.7
298	12.0[b]	97.4	20	1.71−8.03	12.40 ± 1.47	27.6
299	12.0	2.55	13	1.65−5.29	13.13 ± 1.63	32.9
299	12.0	2.55	5.5	1.65−5.29	13.02 ± 1.45	39.9
300	24.0	2.92	13	2.66−9.93	13.39 ± 1.31	38.1
600	12.0[b]	588	2.8	8.82×10^3	$\leq 2.3 \times 10^{-3}$	15.1[c]
600	12.0[b]	3.53×10^4 [d]	1.8	9.95×10^3	$\leq 1.0 \times 10^{-3}$	17.9[c]
600	12.0[b]	3.03×10^3	0.74	9.96×10^3	$\leq 2.3 \times 10^{-3}$	22.3[c]
700	12.0[b]	3.03×10^3	0.74	9.96×10^3	$\leq 2.1 \times 10^{-3}$	32.2[c]

[a] Photolyzing laser intensity (mJ cm^{-2} $pulse^{-1}$). [b] 248-nm photolysis was used (193-nm photolysis was used in all other experiments). [c] Uncoated quartz reactor was used (quartz reactor coated with boron oxide was used in all other experiments). [d] 3-Chloro-1-butene was used as a radical precursor (crotyl bromide was used in all other experiments). [e] Concentrations are in molecules cm^{-3}.

TABLE 2: Conditions and Results of Experiments to Measure the Equilibrium Constants of Reaction (1a,−1a)[g]

										$f \times 10^3$ [c]	
T/K	[He]/10^{16}	[precursor]/10^{11}	L[a]	[O_2]/10^{15}	k_5/s^{-1}	k_{1a}[O_2] / s^{-1}	k_{-1a}/s^{-1}	k_d/s^{-1}	ln(K_p)[b]	trans	cis
345	12.0	3.89	12	0.586	34.0	375.8	25.3	48.5	13.185 ± 0.075	6.41	0.31
350	12.0	3.55	13	0.224	33.7	173.3	73.9	81.1	12.286 ± 0.076	7.01	0.69
350	12.0	4.13	12	0.590	27.9	333.4	40.3	48.8	12.579 ± 0.079	7.01	0.69
355	12.0	74.5	6.4[d]	0.561	16.9	310.5	49.3	23.8	12.343 ± 0.051	7.84	1.38
355	12.0	74.5	24[d]	0.561	25.7	341.4	52.5	36.2	12.375 ± 0.037	7.84	1.38
355	12.0	5240[e]	25[d]	0.562	24.9	343.6	51.2	57.4	12.402 ± 0.080	7.84	1.38
360	12.0	3.34	15	0.467	26.2	280.9	91.0	70.9	11.798 ± 0.065	8.15	1.51
360	12.0	3.89	12	0.992	24.4	423.2	62.7	57.8	11.827 ± 0.077	8.15	1.51
365	6.0	210[f]	1.0	0.801	21.3	242.7	72.0	23.2	11.333 ± 0.033	8.50	1.67
365	6.0	210[f]	0.41	0.801	14.0	209.7	62.3	16.0	11.332 ± 0.095	8.50	1.67
370	12.0	3.00	15	0.856	28.0	306.9	121.5	44.2	10.964 ± 0.063	9.15	2.12
370	12.0	10.8	2.4	0.400	23.4	219.3	138.0	46.2	11.261 ± 0.051	9.15	2.12
370	12.0	10.8	9.9	0.400	26.9	104.9	61.7	21.8	11.328 ± 0.083	9.15	2.12
370	6.0	10.4	6.39	0.377	22.4	180.9	128.5	50.0	11.199 ± 0.054	9.15	2.12
375	12.0	5210[e]	22[d]	0.745	16.0	327.8	151.1	24.6	10.934 ± 0.076	10.04	2.44
375	12.0	5950[f]	53[d]	0.726	8.9	288.6	126.0	0.7	11.017 ± 0.049	10.04	2.44
380	12.0	3.00	15	0.836	26.3	303.2	201.7	39.3	10.441 ± 0.083	11.18	2.75
385	6.0	8.0[e]	8.8	0.727	17.2	138.0	173.2	41.6	9.935 ± 0.072	12.55	3.29
390	12.0	3.89	12	1.01	24.8	198.3	225.3	37.9	9.693 ± 0.074	14.12	4.05

[a] Photolyzing laser intensity (mJ cm^{-2} $pulse^{-1}$). [b] Units of K_p are bar^{-1}. Error limits shown here are the values of relative uncertainty ϵ in the K_1 values (see text). [c] Values of the "correction" function (see text, Section IV.3). [d] 248-nm photolysis was used (193-nm photolysis was used in all other experiments). [e] Crotyl chloride was used as $CH_3CHCHCH_2$ precursor (crotyl bromide or 3-chloro-1-butene were used in all other experiments). [f] 3-Chloro-1-butene was used as $CH_3CHCHCH_2$ precursor (crotyl bromide or crotyl chloride were used in all other experiments). [g] Concentrations are in molecules cm^{-3}.

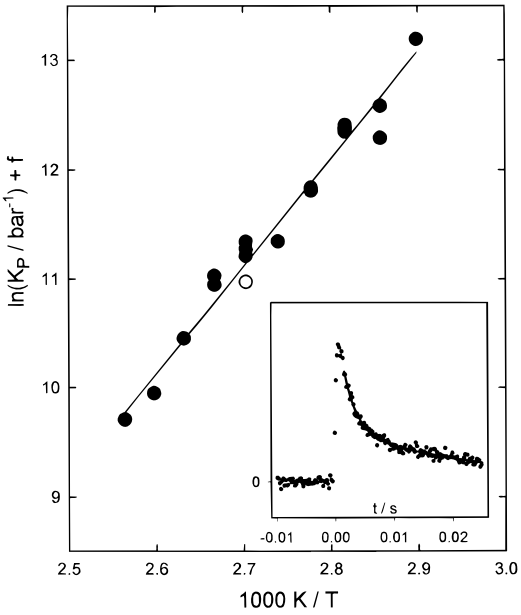

Figure 3. Modified van't Hoff plot of (ln(K_p) + $f(T)$) vs 1000 K/T for reaction (1a,−1a). Line represents the result of the Third Law fit (see text). The insert shows the recorded $CH_3CHCHCH_2$ decay profile (and double-exponential fit) for the conditions of the open plotted point: T = 370 K, [O_2] = 8.562 × 10^{14} molecules cm^{-3}.

One should note that the conditions of the experiments were selected to optimize only the determination of the equilibrium constants. This results in expected high uncertainties of the k_{1a}[O_2], k_{-1a}, and k_d kinetic parameters listed in Table 2, uncertainties that, moreover, are not easily estimated. The values of k_{1a} and k_{-1a} are expected to be in the falloff region which will complicate any potential use of these data. Their temperature dependencies exhibit the anticipated qualitative behavior: k_{-1a} values increase with temperature (as expected for the rate constant of a decomposition reaction) and the values of k_{1a} (corresponding to the second-order addition rate constant) slightly decrease with temperature (as expected for a barrierless addition in the falloff region). The rate constant of the decay of the adduct, k_d, as mentioned above, is interpreted as the rate constant of RO_2 heterogeneous loss. The fitted values of k_d for reaction 1 lie within the range 0.7−81 s^{-1}.

IV. Thermochemistry of Reaction 1a,−1a

The enthalpy changes of reaction (1a,−1a) at room temperature were obtained from the values of $K_1(T)$ using a Third Law analysis. The procedures used have been described before.[10,11,14,16] These calculations require knowledge of the temperature dependencies of the thermodynamic functions (entropy and enthalpy) of the reactants and products of reaction (1a,−1a) which were obtained using the results of ab initio calculations.

IV.1. Interpretation of Experimental Equilibrium Constant Values. Addition of molecular oxygen to the delocalized $CH_3CHCHCH_2$ radical can occur at two positions, terminal

$$CH_3CHCHCH_2 + O_2 \rightleftarrows CH_3{-}CH{=}CH{-}CH_2{-}OO \qquad (1t)$$

and nonterminal

$$CH_3CHCHCH_2 + O_2 \rightleftarrows CH_3{-}C(OO)H{-}CH{=}CH_2 \qquad (1nt)$$

There are two possibilities: (1) addition occurs mainly at one site, either terminal or nonterminal (i.e., rate of addition at the other site is negligible), or (2) addition occurs at both sites with roughly comparable rates. In the first case, the measured rate and equilibrium constants correspond to the process (1t or 1nt) that is nonnegligible. In the second case, however, the observed rate and equilibrium constants need further interpretation and their relationships to the rate parameters of the elementary processes 1t and 1nt needs to be understood.

The reactivity of both terminal and nonterminal sites of CH_3-$CHCHCH_2$ toward O_2 addition is likely to be similar. Atomic spin densities on both corresponding carbon atoms are equal to 1.0 (obtained at UHF/6-31G** level, also see section IV.2). Based on analogy with alkyl radicals, one can expect that steric hindrances to O_2 addition are not likely to result in dramatic differences in the terminal and nonterminal rate constants (rates

of addition of O_2 differ by less than a factor of 3 for *n*-C_3H_7 and *iso*-C_3H_7,[17,18] as well as for *n*-C_4H_9 and *sec*-C_4H_9,[19] and even these differences are explained by correlation with the radical ionization potentials and not steric hindrances[17,19]). Analysis of the experimental equilibrium data obtained in the current work was performed under the assumption that terminal and nonterminal addition rate constants differ by not more than a factor of 3.

Terminal and nonterminal rate constants for the reverse adduct decomposition reaction, −1a, are expected to differ by not more than a factor of 10. Relaxation to equilibrium in the current experimental setup is best observed when k_{-1a} is roughly equal to 100 s^{-1} (corresponding to the middle of the range of temperatures suitable for the determination of equilibrium constants, $T_m \cong 365$ K in the current work). Assuming an Arrhenius dependence for $k_{-1a}(T)$, we estimate that a factor of 10 difference in k_{-1a} values would mean a difference of 7 kJ mol^{-1} in the activation energies for the reverse RO_2 adduct decomposition. In turn, this would mean that T_m values for terminal and nonterminal processes will be separated by ≈35 K. At the same time, the whole temperature interval of the current study where equilibrium was well enough resolved to be suitable for measurements is only 45 K. Thus, one can conclude that rates of the reverse decomposition, k_{-1a}, are different by not more than a factor of 10 for the terminal (1t) and nonterminal (1nt) sites of addition of O_2 to the $CH_3CHCHCH_2$ radical.

If both 1t and 1nt processes are considered, the kinetics of radical decay in the intermediate temperature regime is described by a triexponential expression (corresponding equations are derived in the Supporting Information section IS). However, these triexponential concentration vs time dependencies can be well fitted with a double-exponential expression (I). A computer simulation was performed to assess the relationship between the rate parameters of 1t and 1nt processes and the observed equilibrium constant K_1. Kinetic parameters of individual steps used in the simulation were varied within and slightly outside the ranges observed in the experiments (in s^{-1}): $25 \le k_{1a} \le 400$ and $10 \le k_{-1a} \le 1000$, $0.8 \le K_1[O_2] \le 20$, $0 \le k_d \le 100$ with the above restrictions on the ratios of rate coefficients for the terminal and nonterminal processes. It was found that within these ranges of parameters, modeled triexponential kinetics could be very well fitted with a double-exponential expression I and the resultant value of K_1 is always within a factor of 2 from twice the geometric mean of the actual equilibrium constants for terminal and nonterminal addition:

$$K_1 \cong 2\sqrt{K_{1t}K_{1nt}} \qquad \text{(II)}$$

Thus, experimental values of K_1 provide a measure of the average (arithmetic mean) of ΔG°_T for terminal and nonterminal processes, $\langle \Delta G^\circ_T \rangle_{t,nt}$:

$$\ln({}^1/_2 K_p) \cong \frac{{}^1/_2[\Delta G^\circ_T(1t) + \Delta G^\circ_T(1nt)]}{RT} = \frac{\langle \Delta G^\circ_T \rangle_{t,nt}}{RT} \qquad \text{(III)}$$

where the equality is valid with an accuracy of ±ln(2). Here, K_p is the observed equilibrium constant of reaction (1a,−1a) in bar^{-1}.

IV.2. Molecular Parameters of $CH_3CHCHCH_2$, $CH_3CH(OO)CHCH_2$, and $CH_3CHCHCH_2O_2$. None of the conformations of the species involved in reaction 1 have been investigated before. We studied the geometries and harmonic vibrational frequencies of $CH_3CHCHCH_2$, $CH_3CH(OO)CHCH_2$, and $CH_3CHCHCH_2O_2$ using the ab initio unrestricted HF method with 6-31G** (for $CH_3CHCHCH_2$) and 6-31G* (for peroxy species) basis sets. Internal rotation barriers and cis-trans configuration energies were studied by the MP2/6-31G** method. Geometrical structures corresponding to minima and maxima of the rotational potential energy surfaces were obtained with the full optimization at the UHF level, and the energy was calculated at the MP2/6-31G** level. Structures, vibrational frequencies, and energies of these species are listed in Tables 1S-4S (Supporting Information). The GAUSSIAN 94 system of programs[20] was used in all ab initio calculations.

Cis conformations of $CH_3CHCHCH_2$ and $CH_3CHCHCH_2$-OO were found to be 4.2 (5.1) and 8.0 (8.1) kJ mol^{-1} above the corresponding trans forms. $CH_3CH(OO)CHCH_2$ is 4.2 (4.4) kJ mol^{-1} below *trans*-$CH_3CHCHCH_2OO$ (MP2/6-31G** level, values in parentheses include scaled ZPVE).

The most uncertain aspect of the properties of the radicals pertinent to the calculation of their entropy is the treatment of the hindered internal rotations. In all radicals, $-CH_3$ torsions (periodic triple well) were approximated by a symmetrical ($\sigma = 3$) sinusoidal potential. Potential energy surfaces of other torsional motion in RO_2 radicals have more complex shapes. In the general case, all torsional motions have three unequal minima and three unequal maxima (the only exception is the O1C4C3C2 torsion in *cis*-$CH_3CHCHCH_2O_2$ which has only two minima). In cases when the differences between three maxima are significant, there is an ambiguity in applying sinusoidal approximations (needed to calculate thermodynamic properties) to these complex shapes. One example of such a complex potential is that of the C−OO torsion in cis-$CH_3CHCHCH_2O_2$. This potential has three maxima (11.9, 4.8, and 2.8 kJ mol^{-1} at O2O1C4C3 equal to 1.1°, −128.5°, and 119.2°, respectively) and three minima (at O2O1C4C3 equal to 73.7°, −73.7°, and 172.5°, the second and the third one being 1.39 kJ mol^{-1} above the first one). Two different sinusoidal approximations were used for this potential. One was a single-maximum sinusoida with the barrier height equal to the 11.88 kJ mol^{-1} (two minor maxima are ignored). The other approximation is a 3-fold sinusoida with the barrier height obtained by averaging all three maxima (6.5 kJ mol^{-1}). In such cases, the differences between different possible approximations were taken into account in order to assess the uncertainty in calculating entropy. All energies here are calculated at MP2/6-31G** level with corrections for the zero-point vibrational energy (scaled[21] by a factor of 0.91). Reduced moments of inertia for internal rotations were calculated from the structural data by the method of Pitzer and Gwinn.[22,23] Thermodynamic functions of the hindered internal rotations were obtained from interpolation of the tables of Pitzer and Gwinn.[22] Vibrational frequencies obtained in ab initio calculations were scaled by a factor of 0.89.[21] Properties of the $CH_3CHCHCH_2$, $CH_3CH(OO)CHCH_2$, and $CH_3CHCHCH_2O_2$ radicals used in thermodynamic calculations are listed in Table 3.

IV.3. Determination of ΔH°_{298} and ΔS°_{298} of Reaction (1a,−1a). The room-temperature enthalpy of reaction (1a, −1a) was obtained from the data on $K_1(T)$ using a Third Law analysis. First, the average values of $\langle \Delta G^\circ_T \rangle_{t,nt}$ for terminal and nonterminal processes in reaction (1a,−1a) were obtained directly from the values of the observed equilibrium constant via formula III. The addition of a small "correction"

$$f(T) = \frac{\langle \Delta H^\circ_T \rangle_{t,nt} - \langle \Delta H^\circ_{298} \rangle_{t,nt}}{RT} - \frac{\langle \Delta S^\circ_T \rangle_{t,nt} - \langle \Delta S^\circ_{298} \rangle_{t,nt}}{R} \qquad \text{(IV)}$$

converts the right-hand-side of the equation III to a linear

TABLE 3: Models of the Molecules Used in the Data Analysis

	Vibrational Frequencies (cm^{-1})
trans-$CH_3CHCHCH_2$	197, 272, 472, 495, 666, 698, 826, 909, 949, 989, 1068, 1114, 1199, 1287, 1379, 1424, 1430, 1451, 1459, 2816, 2857, 2892, 2935, 2944, 2945, 3028
cis-$CH_3CHCHCH_2$	267, 274, 487, 537, 634, 697, 812, 906, 970, 990, 1014, 1132, 1154, 1356, 1389, 1398, 1432, 1454, 1464, 2822, 2861, 2915, 2938, 2953, 2962, 3035
$CH_3C(OO)HCHCH_2$	252, 297, 335, 470, 518, 663, 819, 889, 956, 973, 1008, 1061, 1090, 1135, 1170, 1267, 1301, 1317, 1378, 1416, 1441, 1447, 1654, 2845, 2891, 2912, 2921, 2945, 2964, 3023
trans-$CH_3CHCHCH_2OO$	169, 265, 354, 473, 539, 778, 875, 922, 974, 996, 1040, 1057, 1131, 1136, 1253, 1285, 1306, 1369, 1396, 1446, 1454, 1457, 1698, 2847, 2891, 2897, 2919, 2950, 2956, 2979
cis-$CH_3CHCHCH_2OO$	230, 270, 416, 515, 560, 716, 863, 919, 952, 1006, 1013, 1057, 1126, 1132, 1243, 1270, 1337, 1392, 1412, 1448, 1454, 1462, 1692, 2851, 2892, 2901, 2933, 2962, 2974, 2991
CH_2CHCH_2[24]	426, 514, 544, 738, 801, 912, 983, 1071, 1182, 1247, 1390, 1464, 1487, 3019, 3021, 3054, 3107, 3107
CH_2CHCH_2OO[25]	309, 408, 494, 619, 856, 935, 939, 999, 1002, 1109, 1167, 1253, 1285, 1333, 1425, 1453, 1650, 2897, 2951, 3006, 3045, 3103

Rotational Constants (cm^{-1}), Symmetry Numbers (σ, Number of Minima in Parentheses if Different), and Rotational Barriers (kJ mol^{-1})

	Overall Rotations
trans-$CH_3CHCHCH_2$	$B = 0.2749$, $\sigma = 1$
cis-$CH_3CHCHCH_2$	$B = 0.2478$, $\sigma = 1$
$CH_3C(OO)HCHCH_2$	$B = 0.10379$, $\sigma = 1$
trans-$CH_3CHCHCH_2OO$	$B = 0.09865$, $\sigma = 1$
cis-$CH_3CHCHCH_2OO$	$B = 0.10270$, $\sigma = 1$
CH_2CHCH_2[26]	$B = 0.5658$, $\sigma = 2$
CH_2CHCH_2OO[27]	$B = 0.16736$, $\sigma = 1$
	Internal Rotations
trans-$CH_3CHCHCH_2$	$a_1(CH_3-CHCHCH_2) = 6.869$, $\sigma = 3$, $V_0 = 5.04$
cis-$CH_3CHCHCH_2$	$a_1(CH_3-CHCHCH_2) = 5.836$, $\sigma = 3$, $V_0 = 0$
$CH_3C(OO)HCHCH_2$	$a_1(CH_3-C(OO)HCHCH_2) = 5.482$, $\sigma = 3$, $V_0 = 16.55$ $a_2(CH_3C(OO)H-CHCH_2) = 1.508$, $\sigma = 1$ (3), $V_0 = 9.89$ (average of 11.12, 11.10, and 7.45) $a_3(CH_3C(-OO)HCHCH_2) = 1.443$, $\sigma = 1$ (3), $V_0 = 7.43$ (average of 8.35, 10.08, and 3.81; alternative $V_0 = 9.22$)
trans-$CH_3CHCHCH_2OO$	$a_1(CH_3-CHCHCH_2OO) = 5.737$, $\sigma = 3$, $V_0 = 8.39$ $a_1(CH_3CHCH-CH_2OO) = 1.397$, $\sigma = 1$ (3), $V_0 = 8.84$ (average of 10.65, 7.94, and 7.94) $a_1(CH_3CHCHCH_2-OO) = 1.313$, $\sigma = 1$ (3), $V_0 = 6.91$ (average of 10.81, 4.96, and 4.96)
cis-$CH_3CHCHCH_2OO$	$a_1(CH_3-CHCHCH_2OO) = 5.644$, $\sigma = 3$, $V_0 = 3.82$ $a_1(CH_3CHCH-CH_2OO) = 0.638$, $\sigma = 1$, $V_0 = 15.47$ (alternative: $V_0 = 9.57$, average of 15.47 and 3.66) $a_1(CH_3CHCHCH_2-OO) = 1.347$, $\sigma = 1$, $V_0 = 11.81$ (alternative: $V_0 = 6.43$, average of 11.81, 4.73, and 2.76)
CH_2CHCH_2	no internal rotors
CH_2CHCH_2OO[27]	$a_1(CH_2CH-CH_2OO) = 1.785$, $\sigma = 1$ (3), $V_0 = 13.57$ (average of 17.7, 9.6, and 13.4) $a_1(CH_2CHCH_2-OO) = 1.636$, $\sigma = 1$ (2), $V_0 = 8.15$ (average of 5.4 and 10.9; alternative $V_0 = 10.9$)

Entropies Calculated Using the above Models

$S°_{298}$(*trans*-$CH_3CHCHCH_2$) = 304.50 J mol^{-1} K^{-1}
$S°_{298}$(*cis*-$CH_3CHCHCH_2$) = 305.45 J mol^{-1} K^{-1}
$S°_{298}$(*trans*-$CH_3CHCHCH_2OO$) = 378.87 J mol^{-1} K^{-1}
$S°_{298}$(*cis*-$CH_3CHCHCH_2OO$) = 374.03 J mol^{-1} K^{-1}
$S°_{298}$($CH_3CH(OO)CHCH_2$) = 371.10 J mol^{-1} K^{-1}
$S°_{298}$(CH_2CHCH_2) = 258.39 J mol^{-1} K^{-1}
$S°_{298}$(CH_2CHCH_2OO) = 339.54 J mol^{-1} K^{-1}

function of $1/T$ with the intercept at $1/T = 0$ equal to $\langle\Delta S°_{298}\rangle_{t,nt}/R$ and slope of the function equal to $-\langle\Delta H°_{298}\rangle_{t,nt}/R$:

$$\ln(K_p) - \ln 2 + f(T) \cong \frac{\langle\Delta S°_{298}\rangle_{t,nt}}{R} - \frac{\langle\Delta H°_{298}\rangle_{t,nt}}{RT} \quad \text{(V)}$$

Here, angle brackets around thermodynamic functions signify the arithmetic mean of the values for terminal and nonterminal addition of O_2 to $CH_3CHCHCH_2$ (e.g., $\langle\Delta S°_{298}\rangle_{t,nt} = {}^1/_2[\Delta S°_{298,t} + \Delta S°_{298,nt}]$). The equality is valid with an accuracy of $\pm\ln 2$, as in eq III. The values of the "correction" function, $f(T)$, ($\leq 1\%$ of $\ln(K_p)$) were calculated using the models of $CH_3CHCHCH_2$, $CH_3CH(OO)CHCH_2$, and $CH_3CHCHCH_2O_2$ radicals described above (Table 3). The above analysis of thermochemical and equilibrium data was repeated twice: for trans and cis configurations of $CH_3CHCHCH_2$ and $CH_3CHCHCH_2O_2$ which were assumed to be preserved in the addition processes. The resultant values of $f(T)$ are listed in Table 2.

The values of $\Delta S°_{298}$ of reaction (1a,−1a) were calculated using the above models of the involved species (separately for trans and cis configurations):

$$\Delta S°_{298,t}(\text{trans}) = -130.8 \pm 5.6 \text{ J mol}^{-1} \text{ K}^{-1}$$

$$\Delta S°_{298,nt}(\text{trans}) = -138.6 \pm 2.3 \text{ J mol}^{-1} \text{ K}^{-1}$$

$$\Delta S°_{298,t}(\text{cis}) = -136.57 \pm 10.8 \text{ J mol}^{-1} \text{ K}^{-1}$$

$$\Delta S°_{298,nt}(\text{cis}) = -139.50 \pm 2.3 \text{ J mol}^{-1} \text{ K}^{-1}$$

Uncertainties were estimated from the uncertainties in the parameters of the internal hindered rotors (variations in entropy due to different sinusoidal approximations of the torsional potential energy profile and from a 20% uncertainty in the torsional barrier values, see section IV.2) and low-frequency vibrations (estimated by varying the lowest frequency by a factor of 1.5). The values of $\Delta H°_{298}$(trans) and $\Delta H°_{298}$(cis) were obtained from the slopes of the lines drawn through the experimental values of ($\ln(K_p) + f(T)$) and the calculated

TABLE 4: Conditions, Original Results, and Results of the Reinterpretation of the Experiments[5] on the Relaxation to Equilibrium in $CH_2CHCH_2 + O_2 \rightleftarrows CH_2CHCH_2O_2$

T/K	$[O_2]/10^{-5}$ bar	k_w[a]/s^{-1}	λ_1/s^{-1}	λ_2/s^{-1}	F[b]	$k_{6a}[O_2]$/s^{-1}	k_{-6a}/s^{-1}	k_d/s^{-1}	ln(K_P/bar^{-1})(new)[c]	ln(K_P/bar^{-1})(old)[d]	K_P(new)/K_P(dd)	f[e] $\times 10^3$
413	78.22	11.2	1320	18.2	1.20	717.07	585.95	23.98	7.355	7.273	1.086	17.724
411	69.61	11.1	921	11.1	1.05	466.05	443.85	11.10	7.319	7.266	1.054	17.608
401	33.44	10.8	706	13.9	1.27	390.31	302.47	16.32	8.258	8.133	1.133	16.043
391	12.26	11.7	390	10.3	0.805	167.94	212.11	8.55	8.773	8.695	1.082	14.294
382	11.15	10.5	327	8.34	1.27	176.12	142.10	6.62	9.317	9.227	1.094	11.501
373	5.34	11.0	195	9.04	1.12	96.28	89.50	7.25	9.911	9.757	1.166	9.293
372	10.34	11.1	283	7.80	2.12	183.69	89.79	6.22	9.893	9.757	1.146	9.087
363	8.48	12.0	247	8.11	3.50	181.91	54.22	6.97	10.586	10.345	1.272	7.622
362	5.52	12.0	185	8.29	2.31	119.61	55.04	6.63	10.580	10.354	1.254	7.408
354	5.24	14.1	174	6.46	4.39	128.82	32.93	4.62	11.221	10.958	1.300	5.675
353	2.59	14.1	110	6.31	2.40	65.40	34.13	2.68	11.210	11.060	1.162	5.502
352	3.22	11.9	114	7.73	2.85	74.50	29.15	6.18	11.281	10.897	1.469	5.340

[a] Rate constants of the heterogeneous wall decay of CH_2CHCH_2 measured in ref 5. [b] Values of $F = I_1/I_2$ (see section III.3, formula I) reported in ref 5. [c] Values of K_P/bar^{-1} as reported by the authors of the original study. [d] Values of K_P/bar^{-1} obtained in the reinterpretation of the experimental results. [e] Values of the "correction" function (see text).

intercepts $\langle\Delta S^\circ_{298}\rangle/R + \ln 2$ (Figure 3):

$$\langle\Delta H^\circ_{298}\rangle_{t,nt}(\text{trans}) = -82.0 \pm 3.8 \text{ kJ mol}^{-1} \quad \text{(VI)}$$

$$\langle\Delta H^\circ_{298}\rangle_{t,nt}(\text{cis}) = -83.2 \pm 4.7 \text{ kJ mol}^{-1} \quad \text{(VII)}$$

Error limits include contributions resulting from (1) the uncertainties in the entropies of reactions, (2) from the $\pm\ln 2$ uncertainty in equations III and V, and (3) from 2σ of statistical fit of experimental data to eq V. Here, trans and cis notations do not mean enthalpies of reaction (1a,−1a) for corresponding trans and cis conformations of the $CH_3CHCHCH_2$ radical but rather values of reaction enthalpy obtained from experimental data assuming either trans or cis conformations for all radicals. Since values given by expressions VI and VII differ very little, one can recommend the average value for trans and cis routes of reaction (1a,−1a):

$$\langle\Delta H^\circ_{298}\rangle = -82.6 \pm 5.3 \text{ kJ mol}^{-1} \quad \text{(VIII)}$$

A Second Law analysis can be used to obtain both $\langle\Delta H^\circ_{298}\rangle_{t,nt}$ and $\langle\Delta S^\circ_{298}\rangle_{t,nt}$ for reaction (1a,−1a) from the $(\ln(K_p) + f(T))$ vs $1/T$ dependence:

$$\langle\Delta H^\circ_{298}\rangle_{t,nt}(\text{trans, Second Law}) = -81.0 \pm 7.0 \text{ kJ mol}^{-1}$$

$$\langle\Delta S^\circ_{298}\rangle_{t,nt}(\text{trans, Second Law}) = -132.1 \pm 19.2 \text{ J mol}^{-1}\text{ K}^{-1}$$

$$\langle\Delta H^\circ_{298}\rangle_{t,nt}(\text{cis, Second Law}) = -81.1 \pm 7.0 \text{ kJ mol}^{-1}$$

$$\langle\Delta S^\circ_{298}\rangle_{t,nt}(\text{cis, Second Law}) = -132.4 \pm 19.2 \text{ J mol}^{-1}\text{ K}^{-1}$$

(here, error limits are 2σ from statistical deviations of fit only). However, considering the narrow temperature intervals of the experiments to determine $K_1(T)$, the scattering of data due to experimental uncertainties, and effects of the ln2 uncertainty in eqs III and V (potential errors that can have different signs for different data points) we prefer to use the Third Law analysis, based on the ab initio calculated values of entropy.

V. Thermochemistry of Reaction of Allyl Radicals with O_2

Relaxation to equilibrium in the reaction

$$CH_2CHCH_2 + O_2 \rightleftarrows CH_2CHCH_2O_2 \quad \text{(6a,−6a)}$$

was observed by Ruiz et al.,[3] Morgan et al.,[4] and Slagle et al.[5] These studies yielded temperature dependencies of K_6, the equilibrium constants of reaction (6a,-6a), which were used to obtain the enthalpy of the addition of allyl radical to O_2. The experimental method applied by Slagle et al.,[5] laser photolysis/photoionization mass spectroscopy (LP/PIMS), was analogous to the one used in the current work. As has been discussed elsewhere,[10] earlier experiments on relaxation to equilibrium in $R + O_2$ reactions performed by the LP/PIMS method did not account for the possibility of further reaction of the RO_2 (due to wall decay or isomerization/decomposition, also see section III.3) and, therefore, need reinterpretation. Such reinterpretation (described by us earlier[10]) is based on the published parameters of the double-exponential decay of radicals observed in the presence of O_2 and results in corrected values of the equilibrium constants. The conditions of the original experiments on reaction (6a,−6a) by Slagle et al.,[5] the initially reported parameters, and the results of the reinterpretation are listed in Table 4.

As can be seen from the data in Table 4, K_6 increases as a result of the reinterpretation with changes ranging from 5% to 47%. These recalculated K_6 values were used to determine the enthalpy of reaction (6a,−6a) in the Third and Second Law analyses. The entropies of allyl and the $CH_2CHCH_2O_2$ adduct were obtained from spectroscopic and ab initio data on these two radicals (Table 3). In the Third Law analysis, the calculated entropy of reaction (6a,−6a),

$$\Delta S^\circ_{298}(\text{6a,−6a}) = -124.0 \pm 4.5 \text{ J mol}^{-1}\text{ K}^{-1},$$

(uncertainty estimated via the method described in section IV.3) was used together with the experimental (recalculated) $K_6(T)$ data in a procedure described before[10] to obtain the reaction enthalpy

$$\Delta H^\circ_{298}(\text{6a,−6a}) = -76.8 \pm 2.6 \text{ kJ mol}^{-1}$$

Error limits include contributions resulting from (1) the uncertainty in the reaction entropy, (2) from the 25% reported[5] experimental uncertainty in K_6, and (3) from 2σ of statistical fit of experimental data. The same data used in a Second Law analysis yield values of both enthalpy and entropy of reaction (6a,−6a)

$$\Delta H^\circ_{298}(\text{6a,−6a}) = -77.9 \pm 3.2 \text{ kJ mol}^{-1}$$

$$\Delta S^\circ_{298}(\text{6a,−6a}) = -126.8 \pm 8.6 \text{ J mol}^{-1}\text{ K}^{-1}$$

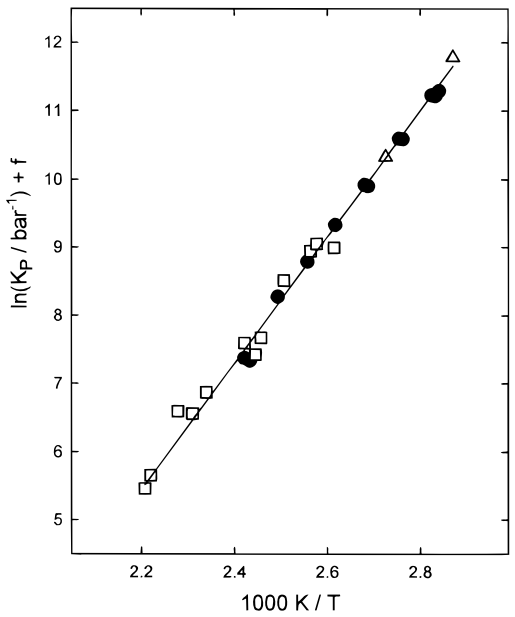

Figure 4. Modified van't Hoff plot of $(\ln(K_p) + f(T))$ vs 1000 K/T for reaction (6a,−6a). Line represents the result of the Third Law fit (see text). Squares: data of Morgan et al.[4] Triangles: data of Ruiz et al.[3] Filled circles: data of Slagle et al.[5] Reinterpreted in the current work (section V).

(here, error limits are 2σ from statistical deviations of fit only) which are in good agreement with those obtained in the Third Law analysis.

Recalculated values of K_6 shown in the modified van't Hoff plot ($\ln K_6/\text{bar}^{-1}$ vs $1/T$, Figure 4) together with the data of Ruiz et al.[3] and Morgan et al.[4] indicate excellent agreement between the results of these three studies. If the data of Ruiz et al. and Morgan et al. are included in the Third and Second Law analyses of thermochemistry, the resultant values are

$$\text{Third Law:}\quad \Delta H^\circ_{298}(6a,-6a) = -77.0 \pm 2.7 \text{ kJ mol}^{-1} \qquad \text{(IX)}$$

$$\text{Second Law:}\quad \Delta H^\circ_{298}(6a,-6a) = -75.8 \pm 2.8 \text{ kJ mol}^{-1}$$

$$\Delta S^\circ_{298}(6a,-6a) = -121.1 \pm 7.0 \text{ J mol}^{-1}\text{ K}^{-1}$$

(reported error limits have the same meaning as above).

The results of the current Third Law and Second Law analyses of the equilibrium in reaction (6a,−6a) are in agreement with those of Morgan et al.[4] Such agreement is expected due to the correspondence between the reinterpreted experimental data of Slagle et al.[5] and those of Ruiz et al. and Morgan et al. (Figure 4).

VI. Discussion

This study provides the first experimental investigation of the thermochemistry of the reaction of 1-methylallyl radical with molecular oxygen. The R−O_2 bond energy (negative of R + ⇄ RO_2 reaction enthalpy) for methylallyl obtained in the experiments on relaxation to equilibrium represents the average of C−O bond energies for terminal and nonterminal addition which are not expected to differ by more than 7 kJ mol^{-1} (see section IV.1). The value of this bond energy, 82.6 ± 5.3 kJ mol^{-1}, is very close to that obtained for the allyl radical, 77.0 ± 2.7 kJ mol^{-1}. Although the value for methylallyl radical is 5.6 kJ mol^{-1} higher, the difference is not meaningful since the uncertainties of the two determinations overlap. Such a weak (compared to alkyl peroxy radicals[10,28]) R−O_2 bond means that, as in the case of allyl radical, the R + ⇄ RO_2 equilibrium is shifted to the left under combustion conditions.

Very little kinetic information on reaction 1 is available in the literature. Stothard and Walker[7] mentioned high yields of butadiene formation among the initial products of 2-butene oxidation at 753 K (with a reference to an unpublished work by the same authors) which they attributed to the importance of the reaction

$$CH_3CHCHCH_2 + O_2 \rightarrow CH_2{=}CHCH{=}CH_2 + HO_2 \qquad \text{(1b)}$$

Earlier, Lodhi and Walker[9] mentioned the value of the reaction 1b rate constant at 753 K being approximately equal to $k_{1b}(753\text{ K}) \cong 3 \times 10^{-16}$ cm^3 molecule^{-1} s^{-1} without giving any reference (presumably, referring to the results of the same unpublished work).

The kinetics and thermochemistry of a prototype reaction, that of the allyl radical with O_2 (6), has received significantly more attention. In addition to the studies of equilibrium in the R + O_2 addition discussed above (section V),[3−5] the high-temperature kinetics of reaction 6 was studied by Walker and co-workers.[6,7,9,29] These authors used gas chromatographic final product analysis of the decomposition of 4,4-dimethylpentene-2 in the presence of O_2[6,9,29] and of the oxidation of propene[7] to assess kinetic parameters of different channels of reaction 6. The reported rate constant values[7] for reaction channels

$$CH_2CHCH_2 + O_2 \rightarrow CH_2{=}C{=}CH_2 + HO_2 \qquad \text{(6b)}$$

and

$$CH_2CHCH_2 + O_2 \rightarrow CO + \text{other products} \qquad \text{(6c)}$$

are $k_{6b}(753\text{ K}) = 4.2 \times 10^{-19}$ cm^3 molecule^{-1} s^{-1} and $k_{6c} = 7.59 \times 10^{-12} \exp(-9457\text{ K}/T)$ cm^3 molecule^{-1} s^{-1}. The overall rate of reaction 6 at high temperatures where equilibrium in the addition channel (6a,−6a) is shifted to the left is, thus, several orders of magnitude lower than typical values for analogous alkyl + O_2 reactions.

Walker and co-workers interpreted reaction channels 6b and 6c as resulting from isomerization of the CH_2CHCH_2OO adduct:

$$CH_2CHCH_2 + O_2 \rightleftarrows CH_2CHCH_2O_2 \rightarrow \text{isomerization} \rightarrow \text{final products}$$

Although reaction 1 is similar to reaction 6, there is a possibility of faster isomerization resulting in higher rate constants of the high-temperature reaction. Terminal addition of $CH_3CHCHCH_2$ to O_2 results in the formation of the $CH_3CHCHCH_2OO$ adduct which can, possibly, isomerize via the abstraction of hydrogen in the allylic position, thus resulting in the formation of a stabilized (due to an electron delocalization) radical by a route similar to that suggested by Baldwin et al.[8] for larger pentenyl radicals:

$$CH_3CHCHCH_2 + O_2 \rightleftarrows CH_3CH{=}CHCH_2OO \rightarrow CH_2CHCHCH_2OOH \rightarrow \text{further products}$$

The activation energy for such an isomerization is expected to be reduced through the formation of the delocalized CH_2-$CHCHCH_2OOH$ radical. However, the upper-limit values for the high-temperature rate constants of reaction 1 obtained in the current work (1×10^{-16} cm^3 molecule^{-1} s^{-1} at 600 K and 2×10^{-16} cm^3 molecule^{-1} s^{-1} at 700 K, in approximate agreement with $k_{1b}(753\text{ K}) \cong 3 \times 10^{-16}$ cm^3 molecule^{-1} s^{-1}

mentioned by Lodhi and Walker) indicate that the above route of reaction 1 is still significantly slower than high-temperature reactions of alkyl radicals with O_2 (e.g., ref 30).

Acknowledgment. This research was supported by the Division of Chemical Sciences, Office of Basic Energy Sciences, Office of Energy Research, U.S. Department of Energy under Grant DE-FG02-94ER1446.

Supporting Information Available: Supplement describing the triexponential kinetics of $CH_3CHCHCH_2$ radical in reaction with O_2. Tables 1S−4S containing information on the properties of $CH_3CHCHCH_2$, $CH_3CH(OO)CHCH_2$, and $CH_3CHCHCH_2O_2$ radicals determined in the ab initio study (24 pages). Ordering information is given on any current masthead page.

References and Notes

(1) Bohm, H.; El Kadi, B.; Baronnet, F. *Oxid. Commun.* **1996**, *19*, 25.
(2) El Kadi, B.; Baronnet, F. *J. Chim. Phys. PCB* **1995**, *92*, 706.
(3) Ruiz, R. P.; Bayes, K. D.; Macpherson, M. T.; Pilling, M. J. *J. Phys. Chem.* **1981**, *85*, 1622.
(4) Morgan, C. A.; Pilling, M. J.; Tulloch, J. M.; Ruiz, R. P.; Bayes, K. D. *J. Chem. Soc., Faraday Trans. 2* **1982**, *78*, 1323.
(5) Slagle, I. R.; Ratajczak, E.; Heaven. M. C.; Gutman, D.; Wagner, A. F. *J. Am. Chem. Soc.* **1985**, *107*, 1838.
(6) Lodhi, Z. H.; Walker, R. W. *J. Chem. Soc., Faraday Trans.* **1991**, *87*, 2361.
(7) Stothard, N. D.; Walker, R. W. *J. Chem. Soc., Faraday Trans.* **1992**, *88*, 2621.
(8) Baldwin, R. R.; Bennett, J. P.; Walker, R. W. *J. Chem. Soc., Faraday Trans. 1* **1980**, *76*, 2396.
(9) Lodhi, Z. H.; Walker, R. W. *J. Chem. Soc., Faraday Trans.* **1991**, *87*, 681.
(10) Knyazev, V. D.; Slagle, I. R. *J. Phys. Chem.* **1998**, *102*, 1770.
(11) Slagle, I. R.; Gutman, D. *J. Am. Chem. Soc.* **1985**, *107*, 5342.
(12) Krasnoperov, L. N.; Niiranen, J. T.; Gutman, D.; Melius, C. F.; Allendorf, M. D. *J. Phys. Chem.* **1995**, *99*, 14347.
(13) Okabe, H. *Photochemistry of Small Molecules*; Wiley: New York, 1978.
(14) Knyazev, V. D.; Bencsura, A.; Dubinsky, I. A.; Gutman, D.; Melius, C. F.; Senkan, S. M. *J. Phys. Chem.* **1995**, *99*, 230.
(15) Bevington, P. R. *Data Reduction and Error Analysis for the Physical Sciences*; McGrow-Hill: New York, 1969.
(16) Knyazev, V. D.; Bencsura, A.; Slagle, I. R. *J. Phys. Chem.* **1998**, *102*, 1760.
(17) Ruiz, R. P.; Bayes, K. D. *J. Phys. Chem.* **1984**, *88*, 2592.
(18) Atkinson, R.; Baulch, D. L.; Cox, R. A.; Hampson, R. F., Jr.; Kerr, J. A.; Troe, J. *J. Phys. Chem. Ref. Data* **1992**, *21*, 1125.
(19) Lenhardt, T. M.; McDade, C. E.; Bayes, K. D. *J. Chem. Phys.* **1980**, *72*, 304.
(20) Frisch, M. J.; Trucks, G. W.; Schlegel, H. B.; Gill, P. M. W.; Johnson, B. G.; Robb, M. A.; Cheeseman, J. R.; Keith, T.; Petersson, G. A.; Montgomery, J. A.; Raghavachari, K.; Al-Laham, M. A.; Zakrzewski, V. G.; Ortiz, J. V.; Foresman, J. B.; Cioslowski, J.; Stefanov, B. B.; Nanayakkara, A.; Challacombe, M.; Peng, C. Y.; Ayala, P. Y.; Chen, W.; Wong, M. W.; Andres, J. L.; Replogle, E. S.; Gomperts, R.; Martin, R. L.; Fox, D. J.; Binkley, J. S.; Defrees, D. J.; Baker, J.; Stewart, J. P.; Head-Gordon, M.; Gonzalez, C.; Pople, J. A. *Gaussian 94*, Revision E.1; Gaussian, Inc.: Pittsburgh, PA, 1995.
(21) Pople, J. A.; Scott, A. P.; Wong, M. W.; Radom, L. *Isr. J. Chem.* **1993**, *33*, 345.
(22) Pitzer, K. S.; Gwinn, W. D. *J. Chem. Phys.* **1942**, *10*, 428.
(23) Pitzer, K. S. *J. Chem. Phys.* **1946**, *14*, 239.
(24) Liu, X.; Getty, J. D.; Kelly, P. B. *J. Chem. Phys.* **1993**, *99*, 1522.
(25) Baskir, E. G.; Nefedov, O. M. *Russ. Chem. Bull.* **1996**, *45*, 99.
(26) Hirota, E.; Yamada, C.; Okunishi, M. *J. Chem. Phys.* **1992**, *97*, 2963.
(27) Boyd, S. L.; Boyd, R. J.; Shi, Z.; Barclay, L. R. C.; Porter, N. A. *J. Am. Chem. Soc.* **1993**, *115*, 687.
(28) Pilling, M. J.; Robertson, S. H.; Seakins, P. W. *J. Chem. Soc., Faraday Trans.* **1995**, *91*, 4179.
(29) Baldwin, R. R.; Lodhi, Z. H.; Stothard, N.; Walker, R. W. *Proc. Int. Symp. Combust.* **1990**, *23*, 123.
(30) Wagner, A. F.; Slagle, I. R.; Sarzynski, D.; Gutman, D. *J. Phys. Chem.* **1990**, *94*, 1853.